

Bandwidth Enhancement of Silicon Traveling-Wave Modulators Using Distributed Micro-Capacitors

Abdolkhalegh Mohammadi^(1,2), Leslie A. Rusch^(1,2), Wei Shi^(1,2)

⁽¹⁾ Department of Electrical and Computer Engineering and ⁽²⁾ Center for Optics, Photonics, and Lasers (COPL), Université Laval, Québec, QC, Canada. wei.shi@gel.ulaval.ca

Abstract We present a novel technique for enhancing the bandwidth of a silicon traveling-wave modulator by incorporating micro-capacitors distributed along its electrode. A bandwidth of 61 GHz is achieved, substantially higher than a conventional design (45 GHz) with a comparable V_π .

©2023 The Author(s)

Introduction

The development of optical interconnects toward higher transmission data rates has led to the growing demand for higher modulator bandwidth. Silicon photonics is a prominent technology for optical transceivers because of advantages such as small size, CMOS compatibility, and low cost. Recent advances in silicon photonic modulators have achieved very high bandwidths such as microring modulators (MRMs) with a bandwidth of 110 GHz (using optical peaking) and 240 Gb/s PAM-8^[1], and slow-light modulators with a bandwidth of greater than 100 GHz and 110 Gbps OOK^[2]. These results show the great potential of silicon photonics for very high data-rate transmission. Nevertheless, these resonator-based devices confront challenges of narrow optical bandwidth, sensitivity to temperature variation, and low power handling capacity^[3]. To date, traveling-wave Mach-Zehnder modulators (TW-MZMs) are still the most popular in practical applications thanks to their robustness and easy operation. A 67-GHz bandwidth has recently been demonstrated for a segmented TW-MZM^[4]. However, achieving such a high bandwidth required a very short segment (2 mm in the reference^[4]), leading to a high single-segment V_π (about 14 V).

It has been shown that the bandwidth of the silicon TW-MZM depends on microwave attenuation along its traveling-wave electrode loaded by the PN junction in the doped silicon waveguide^{[5],[6]}. The microwave attenuation increases quickly with the distributed capacitance in an RF transmission line, which is normally dominated by the junction capacitance in the silicon TW-MZM.

In this work, we propose a novel traveling-wave electrode design with vertical metal micro-capacitors connected in series to the PN-junction to reduce the overall distributed capacitance.

Using this technique, we have substantially increased the bandwidth by more than 30% (from 45 GHz to 61 GHz) with an only slightly increased V_π for a silicon TW-MZM fabricated using a standard silicon photonic foundry process.

Design and Fabrication

The schematic of our proposed micro-capacitor (MC) enhanced TW-MZM is shown in Fig. 1. It consists of two depletion-type phase shifters using the free-carrier plasma dispersion effect, which have a length of 4 mm and are connected in the series push-pull configuration driven by a TW electrode. The TW electrode (the hashed area) has a coplanar strip (CPS) structure with periodic T-shaped extensions to reduce the velocity of the microwave signal to match that of the optical wave. The design of the silicon phase shifter and the CPS follow the procedure explained comprehensively in our previous works^[5]. As observed in the 3D model of the phase shifter in Fig. 1, three levels of doping have been used for the PN-junction in a silicon rib waveguide that is 220-nm height. To lower the resistance of the PN-junction for higher bandwidth, an intermediate doping level (N+, P+) is applied. The PN junction and electrodes have ohmic contact by use of a highly doped level (N++, P++). At the input of the MZM, an adjustable coupler using two metal heaters balances the input power between the MZM arms for a better extinction ratio.

The distributed micro-capacitors along the TW electrode are designed in the vertical direction with two metal layers (M1 and M2 in Fig.1). A series of identical T-shaped extensions (each 47 μm in length) are designed in both metal layers that are connected through a via (VIA2 in Fig.1) for every other T-shaped extension. The PN junction underneath is segmented with the same size

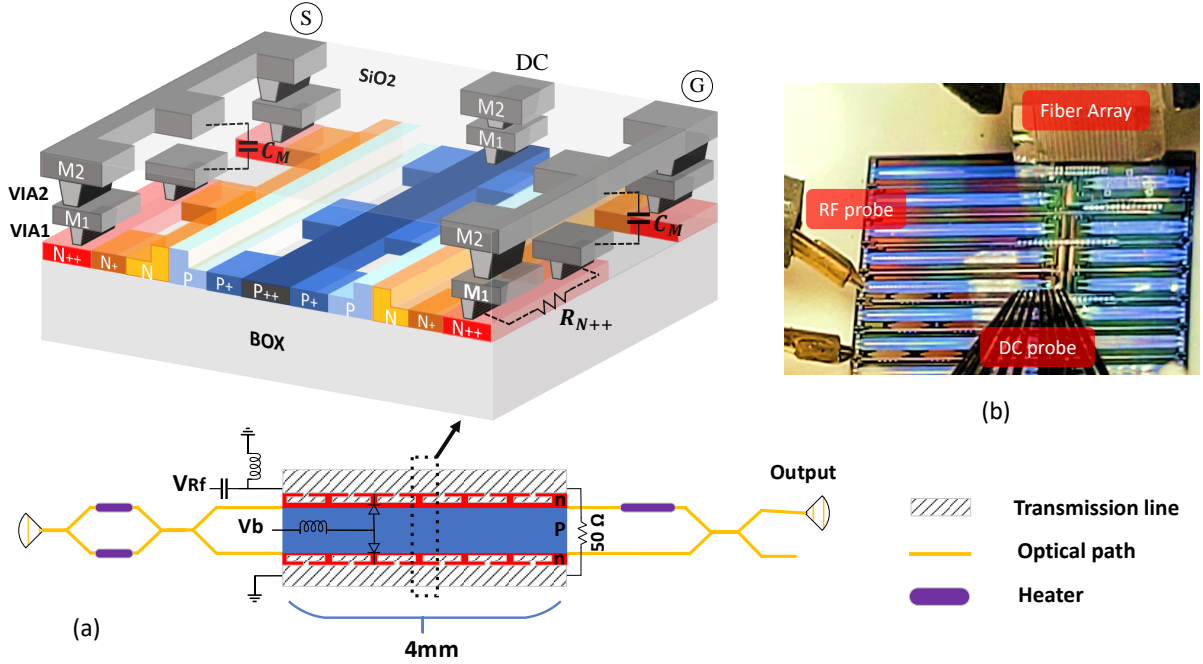


Fig. 1: Left: Schematic of the designed modulator (inset: 3D model of the phase shifter). Right: Photo of the chip under test

as these T-shaped extensions. Those pairs of T-shaped extensions without the via connection effectively form small capacitors that are connected in series with the capacitance of the junction segments. Using this technique, we reduce the total loaded capacitance to about 70% of its value. Note that the electrodes are in the top metal (M2). Additionally, we electrically connect the adjacent junction segments with and without the micro-capacitors in the heavily doped silicon slab (N++ and P++) with very low resistance. This assures the PN junction connected to the micro-capacitors can be effectively charged at DC and low frequencies and thus maintain the modulation efficiency. For comparison, we also designed a conventional TW-MZM where M1 and M2 are connected for all the junction segments. Both devices were fabricated on the same wafer using a 200-mm-wafer silicon photonics foundry process. Figure 1(b) shows the fabricated chip under test. We will see later that the two designs have almost the same V_{π} .

Simulation and Analysis

Figure 2 shows the simulated electro-optic response (S21) of the conventional 4mm TW-MZM and the MC-enhanced TW-MZM using a time-domain numerical model^[7]. The propagation constant and the characteristic impedance of the unloaded CPS electrodes are numerically calculated using the finite element method in ANSYS HFSS. The conventional TW-MZM (CON) has an E-O bandwidth of 27.5 GHz and 46.5 GHz when

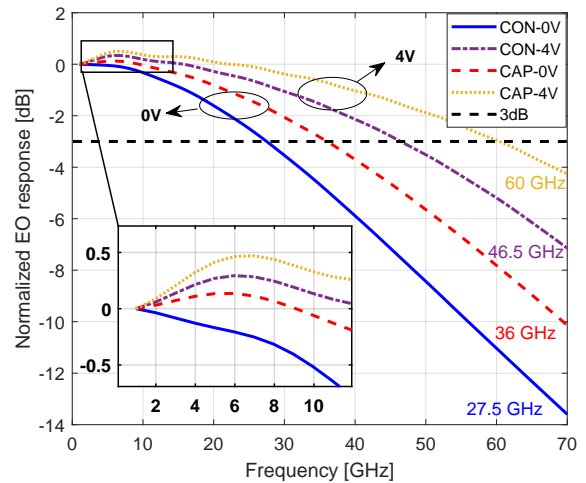


Fig. 2: EO response simulation for conventional 4mm MZM (CON) and integrated micro-capacitance (CAP) one at 0V and 4V.

reversely biased at zero and 4V, respectively. Using the integrated micro-capacitors (CAP), the simulation predicts a bandwidth of 36 GHz and 60 GHz at 0V and 4V, respectively, indicating greater than 30% enhancement. Small peaks are observed at frequencies near 5 to 10 GHz for both designs, which are attributed to the variation of the characteristic impedance of the TW electrodes. In other words, the impedance mismatch between the TW electrode and the 50-ohm termination leads to slight impedance peaking.

To better understand the principle, we show an equivalent circuit model of one junction segment for the conventional (Fig. 3a) and MC-enhanced design (Fig. 3b). The junction segment is very short ($< 50 \mu\text{m}$) so that we can treat all the el-

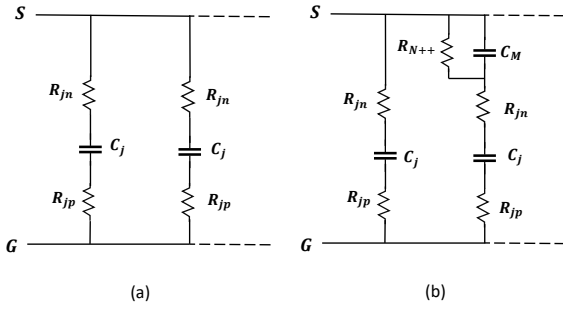


Fig. 3: a) Equivalent circuit of the conventional TW-MZM, b) Equivalent circuit of the TW-MZM with MC-enhanced design.

elements as lumped. In Fig. 3, C_j , R_{jn} , and R_{jp} stand for junction capacitance and resistances (in N and P doped silicon), respectively, and C_M and R_{N++} are the integrated vertical micro-capacitor and the resistor through the heavily doped slab. We can see that C_M is connected in series to the P-N junction capacitance (C_j). It was shown that adding a serial RC equalizer increases the cut-off frequency of a forward-biased PIN modulator with a lumped electrode^[8]. In our design, the adding of C_M along the TW electrode reduces the total capacitance loaded to the transmission line and thus leads to a lower microwave loss and ultimately a higher bandwidth.

DC and RF Characterization

DC characterization of the phase shifter shows a $V_\pi L$ of about 3 V·cm. Figure 4 shows the normalized optical power varied with applied DC voltage. We can observe a V_π of 7.5 V for the conventional design and a lightly higher value (about 8.3 V) for the MC-enhanced TW-MZM. Figure 5 shows the measured electro-optic responses of the conventional TW-MZM (CON) and MC-enhanced TW-MZM (CAP) at zero and 4 V reverse biases. These results were obtained using a vector network analyzer (VNA - Keysight N5227A) and a 70-GHz photo-detector. In comparison to the conventional design, the MC-enhanced TW-MZM shows a bandwidth substantially increased from 28 GHz to 36 GHz at zero bias and from 45 to 61 GHz at 4 V reverse bias. We also observe good agreement between the measurement and simulation results (Fig. 2).

Conclusion

We have proposed and demonstrated a novel silicon TW-MZM using distributed micro-capacitors. We showed that utilizing the distributed micro-capacitors connected to the PN-junctions along the TW electrode can substantially increase the bandwidth while maintaining a V_π comparable to the conventional design.

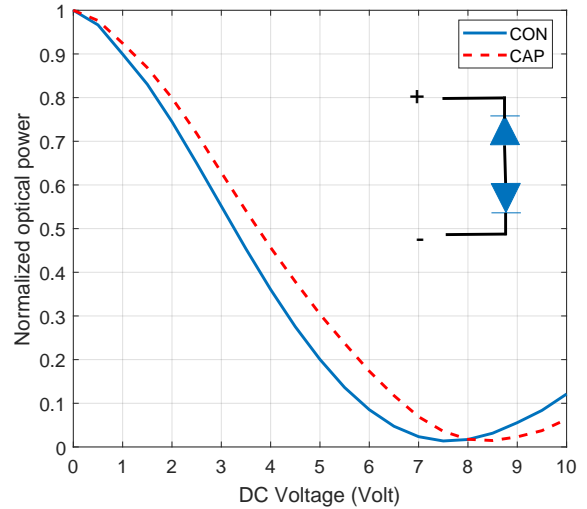


Fig. 4: Measured optical power transmission as a function of applied DC voltage on the conventional TW-MZM (CON) and the micro-capacitor enhanced TW-MZM (CAP).

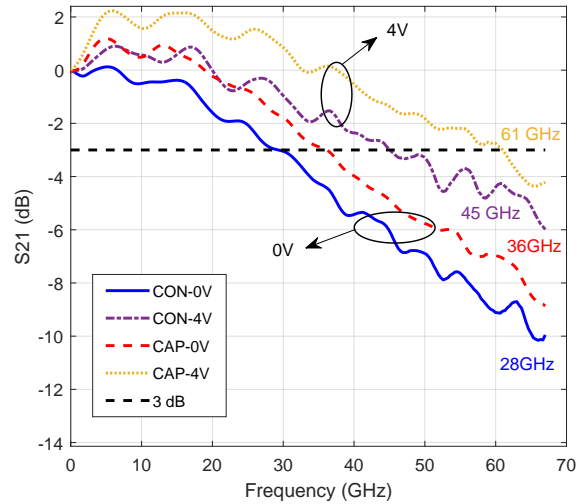


Fig. 5: Measured EO responses of the conventional TW-MZM (CON) and micro-capacitance enhanced TW-MZM one (CAP) reversely biased at 0V and 4V.

Acknowledgements

We thank S. Levasseur and N. Bacon for their technical support. The chip was fabricated via CMC Microsystems. This project is funded by Huawei Canada and NSERC (CRDPJ528381).

References

- [1] Y. Zhang, H. Zhang, J. Zhang, *et al.*, "240 Gb/s optical transmission based on an ultrafast silicon microring modulator", *Photon. Res.*, vol. 10, no. 4, pp. 1127–1133, Apr. 2022. DOI: 10.1364/PRJ.441791. [Online]. Available: <https://opg.optica.org/prj/abstract.cfm?URI=prj-10-4-1127>.
- [2] C. Han, M. Jin, Y. Tao, B. Shen, H. Shu, and X. Wang, "Ultra-compact silicon modulator with 110 GHz bandwidth", in *Optical Fiber Communication Conference (OFC) 2022*, Optica Publishing Group, 2022, Th4C.5. DOI: 10.1364/OFC.2022.Th4C.5. [Online]. Available: <https://opg.optica.org/abstract.cfm?URI=OFC-2022-Th4C.5>.

- [3] M. De Cea, A. H. Atabaki, and R. J. Ram, "Power handling of silicon microring modulators", *Optics express*, vol. 27, no. 17, pp. 24 274–24 285, 2019.
- [4] A. Mohammadi, Z. Zheng, J. Lin, *et al.*, "Segmented silicon photonic modulator with a 67-GHz bandwidth for high-speed signaling", in *Optical Fiber Communication Conference (OFC) 2022*, Optica Publishing Group, 2022, Th3C.1. DOI: 10 . 1364 / OFC . 2022 . Th3C . 1. [Online]. Available: <https://opg.optica.org/abstract.cfm?URI=OFC-2022-Th3C.1>.
- [5] H. Sepehrian, J. Lin, L. A. Rusch, and W. Shi, "Silicon photonic IQ modulators for 400 Gb/s and beyond", *Journal of Lightwave Technology*, vol. 37, no. 13, pp. 3078–3086, 2019. DOI: 10.1109/JLT.2019.2910491.
- [6] A. Mohammadi, Z. Zheng, X. Zhang, L. A. Rusch, and W. Shi, "Segmented silicon modulator with a bandwidth beyond 67 GHz for high-speed signaling", *Journal of Lightwave Technology*, pp. 1–8, 2023. DOI: 10 . 1109 / JLT . 2023 . 3250112.
- [7] H. Bahrami, H. Sepehrian, C. S. Park, L. A. Rusch, and W. Shi, "Time-domain large-signal modeling of traveling-wave modulators on soi", *Journal of Lightwave Technology*, vol. 34, no. 11, pp. 2812–2823, 2016. DOI: 10.1109/JLT.2016.2551702.
- [8] T. Baba, S. Akiyama, M. Imai, and T. Usuki, "25-Gb/s broadband silicon modulator with 0.31-VCm V_{π} .L based on forward-biased pin diodes embedded with passive equalizer", *Opt. Express*, vol. 23, no. 26, pp. 32 950–32 960, Dec. 2015. DOI: 10 . 1364 / OE . 23 . 032950. [Online]. Available: <https://opg.optica.org/oe/abstract.cfm?URI=oe-23-26-32950>.